PERFORMANCE OPTIMIZATION OF COMMERCIAL PHOTOVOLTAIC TECHNOLOGIES UNDER LOCAL SPECTRAL IRRADIANCES USING MACHINE LEARNING

MANJEEVAN SINGH SEERA

A project report submitted in partial fulfilment of the requirements for the award of the degree of Masters of Engineering (Electrical)

Lee Kong Chian Faculty of Engineering and Science
Universiti Tunku Abdul Rahman

January 2018

DECLARATION

I hereby declare that this project report is based on my original work except for citations and quotations which have been duly acknowledged. I also declare that it has not been previously and concurrently submitted for any other degree or award at UTAR or other institutions.

Signature : ___________________________

Name : Manjeevan Singh Seera

ID No. : 17UEM01232

Date : 24 April 2018

APPROVAL FOR SUBMISSION

I certify that this project report entitled **"PERFORMANCE OPTIMIZATION OF COMMERCIAL PHOTOVOLTAIC TECHNOLOGIES UNDER LOCAL SPECTRAL IRRADIANCES USING MACHINE LEARNING"** was prepared by **MANJEEVAN SINGH SEERA** has met the required standard for submission in partial fulfilment of the requirements for the award of Masters of Engineering (Electrical) at Universiti Tunku Abdul Rahman.

Approved by,

Signature : ___________________________

Supervisor : Prof. Dr. Chong Kok Keong

Date : 24 April 2018

ACKNOWLEDGEMENTS

First and foremost, I offer my sincerest gratitude to my supervisor, Prof. Dr. Chong Kok Keong who has supported me throughout my thesis with his patience, motivation and knowledge. One simply could not wish for a better or friendlier supervisor. My sincere thanks go to Aaron Hong for his assistance in the equipment setup. My wife and my parents provided countless support, which was much appreciated.

PERFORMANCE OPTIMIZATION OF COMMERCIAL PHOTOVOLTAIC TECHNOLOGIES UNDER LOCAL SPECTRAL IRRADIANCES USING MACHINE LEARNING

ABSTRACT

The irradiance from the sun or solar spectral can have significant variance in different locations due to the latitude, humidity, cosine effect of incident sunlight. Performance of the outdoor photovoltaic (PV) modules is greatly influenced by the spectrum. In this study, the effects of the local spectral irradiance on outdoor PV modules is of interest. With similar irradiance and operating temperature, the performance of the PV modules at different locations differ as compared with the benchmark AM1.5G results. In order to predict the actual PV module performance under local climate conditions, a total of five locations in Peninsular Malaysia are considered. Twelve solar PV modules from different manufacturers and materials are analysed. Two sets of experiments were conducted using variants of Genetic Algorithms, where the PCE at different irradiance levels is first taken into account. Then, a multi-objective problem involving several parameters of the solar module is considered. Results from the study show that there is a gap from the AM1.5G results with the results from the five locations being analysed.

TABLE OF CONTENTS

LIST OF TABLES

LIST OF FIGURES

CHAPTER 1

INTRODUCTION

1.1 Background

Renewable energy consists of various systems from solar photovoltaic (PV), wind turbines, to tidal energy. Solar PV has been one of the most popular options, due to its simplicity of harvesting energy that is abundant from the sun. It is especially viable in rural electrification and proved to be a cost-efficient way to electrify rural areas in developing countries (Ma et al., 2017). Demand for the solar PV systems has risen over the years as a method in reducing the dependency of using fossil fuels. There has been a constant increase of investments, from both the government and private sector in terms of research for better and cheaper solar modules and systems, and the use of more solar PV systems (Ma et al., 2017).

It is impossible to measure solar irradiance for every location on earth. Studies have been done to model average solar irradiance over broad geographical areas (Norton et al., 2017). This information, however, does not go into detail by states or even cities. To extract valuable trends in data, it is helpful to classify each spectrum using a single metric that is able to balance short and long wavelengths, in relation to the Standard Test Conditions (STC) (Norton et al., 2017).

Effect of the difference in spectral irradiance in regards to the performance of solar cells is well known by the international community for solar energy. The efficiency and power output of PV modules under solar irradiance is typically lower than the rated STC. Other than STC, there is another standard used, which is known as nominal operating conditions (NOC). Values of STC and NOC for irradiance are 1000 W/m^2 and 800 W/m^2, ambient temperature 25° C and 20° C, respectively, with a wind speed of 1 m/s for NOC.

To date, the impact of different spectral irradiances on the PV modules is mainly weighted based on two widely used parameters: average photon energy (APE) and spectral mismatch factor (SMF), which can be seen from numerous studies worldwide. In general, APE is used in classifying solar irradiance from the relative energy distribution, over spectrum (Norton et al., 2017). The work in Norton et al. (2017) looks into comparing global spectral distributions from two separate locations, which are indexed using APE. APE can be seen as a good predictor of spectral irradiance for both datasets after low irradiance data was filtered (Norton et al., 2017). In Horio et al. (2017), the value of APE changes the I_{sc} of PV modules, which have possibilities of I_{sc} correction using APE coefficient. Similar to Horio et al. (2017), I_{sc} correction is possible using the APE index in Mano et al. (2017). In Nofuentes et al. (2017), it is noted that APE does not represent the uniqueness of the complete spectrum.

The influence of spectrum variations on perovskite solar cells performance was considered in Senthilarasu et al. (2015) under various atmospheric conditions. Spectrum losses by the solar cells under various climatic conditions are crucial for the solar cell community to increase the stability (Senthilarasu et al., 2015). Impact on varying spectrum irradiance for various PV technologies was made in Dirnberger et al. (2015). Results show that APE did not represent the advantages over spectral mismatch factor, and it should be used for qualitative evaluations only (Dirnberger et al., 2015).

While STC is typically presented by manufacturers, they do not represent the actual climatic conditions around the world (Ishii et al., 2011). No complete information about the energy performance of the PV is given at the installation site (De Soto et al., 2006). In this case, it is essential to know the energy produced under actual operating conditions are essential for return-on-investment. In this context, it is essential to monitor and evaluate PV system’s operating performance under local conditions as it assists the users to utilize the electricity fully.

Not only local conditions matter, the type of material used by the solar module matter. This is due to solar cells respond differently to spectrum at different wavelength range (Sirisamphanwong & Ketjoy, 2012). As an example solar cells respond differently at different wavelength ranges, i.e., spectrum responses of a-Si and p-Si spectrum response is 305–820 nm and 305–1200 nm, respectively (Sirisamphanwong & Ketjoy, 2012). Though spectrum response of a-Si is smaller than p-Si, the spectrum irradiance has a more significant energy response with a-Si (Sirisamphanwong & Ketjoy, 2012). Outputs of Si PV depend on the module temperature while in thin-film ones, it depends both on spectrum distribution and module temperature (Minemoto et al., 2009).

In recent years, Genetic Algorithms or better known as GA, have been commonly used in the domain of solar PV. GAs are typically used in generating right solutions to optimize and search problems. Improvements of a dynamic electric battery model are made using an automated parameter extraction using GA in Blaifi et al. (2016). The proposed GA model in Blaifi et al. (2016) shows an agreement with actual measurements in different modes and conditions. An enhanced evolutionary computing model was used in Kumari and Geethanjali (2017) to extract PV design parameters using an adaptive GA. The curve fitting for I-V was used to find the optimal PV parameters. Identifying single-diode model in PV generators under outdoor conditions was done in Bastidas-Rodriguez et al. (2017). Non-linear equations in five different operating points were written to be optimized using GA. Parameters of a single hybrid channel PV thermal module were optimized in Singh et al. (2015). Optimization was done using GA, where the efficiency for thermal and electrical was optimized. A maximum power point tracking (MPPT) model using a modified GA was done in Daraban et al. (2014). Integrating an MPPT algorithm in the GA structure made finding the maximum power point faster by decreasing the number of iterations.

1.2 Objectives of the Project

The objectives of this research study are as follow:

- To collect local solar irradiance data from various locations in Peninsular Malaysia;
- To optimize the performance of the various photovoltaic cells using machine learning;
- To evaluate the best performing photovoltaic technology in given conditions under local spectral irradiances.

1.3 Problem Statement

There is a gap between the results of solar PV in the datasheets and the performance of the actual site. The results in the datasheets are based on laboratory test results under the standard air mass 1.5 condition, known as AM1.5G. As spectral irradiance varies from location, and even by city, taking the standard AM1.5G is not a good reference point. Performance of different materials, such as monocrystalline silicon and polycrystalline silicon and highly dependent on the spectral response. It is a challenging question in determining for any of these technologies if it is suitable for specific climate conditions. In this study, the research question is:

> *"How to determine the most suitable PV technology under local spectral irradiance to save time and money?"*

1.4 Research Work

Understanding how the outdoor performance of solar PV modules with factors such as the environment is crucial in developing energy ratings. The Malaysian climate is humid and hot with high ambient temperature. It has indirectly affected the local solar spectral irradiance, which is much different from conventional standard AM 1.5. In this research, the local solar irradiance data will be acquired and compared with standard irradiance AM 1.5. Detailed analysis will be done using computer software, to analyse the performance of various types of commercially available PV devices to obtain the most suitable types for different locations in Malaysia.

In the work of Chong et al. (2016), the efficiency of power conversion under different spectral irradiances for organic solar cells was of interest. In this study, a relatively comprehensive methodology based genetic algorithm to obtain the most optimized performances of various commercial PV modules under local locations. While APE and SMF have been used by other literature, there is no reported work on using local spectrum information to commercial PV modules.

As such, the primary contribution in this thesis is to bridge the gap between the information provided by the PV manufacturer in the datasheet with the actual spectrum at various locations, to get a reasonable estimate of the output power. There are two new knowledge to be added in the current literature gap:

(1) the use of local spectrum in various locations in Malaysia, which gives a better understanding of PV performance, and

(2) the use of genetic algorithms in optimizing the efficiency rates of the solar modules.

CHAPTER 2

LITERATURE REVIEW

In this section, a review of the various literature, which includes GA and EA is done. The areas of focus are on solar PV, PV thermal (PVT), concentrated PV (CPV), and PV hybrid.

2.1 Solar PV

An adaptive GA was used for to extract design parameters for solar PV in Kumari and Geethanjali (2017). The I-V curve fitting method was used in locating optimum PV parameters. The curve fits well at various irradiation levels which enables the use of optimum PV parameters, as compared to standard approaches.

Basis GA (BGA) and segmented GA (SGA) was used in Cortés et al. (2018) to optimize electricity costs and heating networks in the building. The aim is to get the best energy source configurations to meet electric and heating demands in a period of fifteen minutes, which in turn reduces operating costs. SGA shows to be better than BGA in regards to convergence and quality of solutions.

Accurate modelling of PV modules was done in Muhsen et al. (2015) using differential evolution with integrated mutation per iteration (DEIM). Modelling of PV module is done for extracting various parameters such as weather condition photocurrent, diode ideality factor, shunt and series resistance, and diode ideality factor. DEIM shows good accuracy with fast convergence speed, compared to other methods.

Distributed EA was used in Bucking and Dermardiros (2018) for an integrated community energy system by optimizing building design and district technology. The objective is to achieve a renewable energy balance in the building. In a commercial office, it shows that isolated optimization as compared to community integrated optimization can be scaled for future community master planning studies.

In the estimation of single-diode PV module parameters, EA is used in Muhsen et al. (2016), while GA is used in Bastidas-Rodriguez et al. (2017). In Muhsen et al. (2016), the objective was to optimize PV currents. The results showed that EA had the advantage of estimating accurately, converging rapidly, and with fewer control parameters. In Bastidas-Rodriguez et al. (2017), objective involving PV source in five operating points is solved using GA. The single-diode model parameters are evaluated in combinations of two conditions, i.e., irradiance and temperature. Compared to other models, the analysis indicates that parameters require being changed in regards to environmental conditions in order to reduce error for power, current, and energy predictions.

In ensuring maximum power is produced in real irradiance conditions, EA is used in Carotenuto et al. (2015). The objective was to optimize the output power, with results show convergence capabilities of EA, and minimizes computation time.

In improving the dynamic model of battery for PV, GA is used in Blaifi et al. (2016). Extraction of parameters using GA provides lower error rates and better matching with actual measurements, as compared with other models. The model is noted to be more accurate for various battery types in many conditions.

In determining the best options to reduce net building energy cost and increase PV utilization efficiency, GA is utilized in Youssef et al. (2016). The objectives are to meet the dimension of the building, the ratio from wall-to-wall, and placement integration of PV. Results show the optimum envelopes with the best location for building integrated PV from energy and economic point of view.

GA is used in an array of module arrangement to reduces mismatch losses for PV in Shirzadi et al. (2014). GA locates the best arrangement of modules in the array, taking into account the output power from the array to be maximized. Results indicate the potential of energy savings, at several irradiations and temperature levels.

PV parameters are identified and optimized using a hybrid GA in Rong et al. (2015). The objectives are to improve the identification accuracy for those results with a more substantial error. By comparing the predicted results with the measured results, it proves the effectiveness of the method.

In the quest to track global maximum power point (MPP) in PV system affected by partial shading, a modified GA is proposed in Daraban et al. (2014). Results show that the modified GA optimizes the parameters with an excellent final solution.

In predicting PV electrical performance, Tabu Search with differential evolution is used in Siddiqui and Abido (2013). The objective is the sum of the slope of the power–voltage curve and the errors in current predictions at short circuit, open circuit and maximum power points. Results show that the algorithm gives lowest objective values, and it is more accurate as compared to other algorithms.

2.2 PVT

In improving PVT efficiency system in India, GA is used in Singh et al. (2015b). The objectives are to improve both thermal and exergy efficiency. Results show an improvement in exergy and thermal efficiencies during the optimization process.

Design parameters of transparent PVT system are optimized in Singh and Agrawal (2015) using GA with fuzzy. The objectives of increasing the total exergy efficiency. Results show that GA with fuzzy system converges faster as compared to standard GA models.

A fuzzified GA is used in Singh and Agrawal (2016) on a hybrid dual channel semitransparent PV thermal module. The objectives are the same as Singh and Agrawal (2015), with results showing average improvement in electrical efficiency in the module that has been optimized.

A single-channel glazed PVT is optimized with EA in Singh et al. (2015). Evaluating overall exergy and thermal gains annually, results show that optimization using EA shows an improvement in the overall gains.

2.3 CPV

CPV, or concentrator photovoltaic is used in Arias-Rosales and Mejía-Gutiérrez (2018) and Burhan et al. (2016). In Arias-Rosales and Mejía-Gutiérrez (2018), a GA-Weibull Arias algorithm is used in optimizing effective concentration, material cost, and total space. The outcome is an efficient and flexible tool for determining the solar V-Troughs setup in various scenarios.

In Burhan et al. (2016), sunlight irradiance beam is harnessed to change the electricity converted into Hydrogen/Oxygen gas. A micro GA model is used in optimizing the configuration and size in the proposed CPV-Hydrogen system. The goal is to have no failure time for the power supply and to have the overall system cost to be minimum.

2.4 Hybrid PV

GA is used in Paulitschke et al. (2017) to optimize energy for household using PV and fuel cell. The objectives are to reduce the amount of power, in which the fuel cell and battery can be used together in order to boost the lifespan.

EA is used in Jiménez-Fernández et al. (2014) to optimize a PV-hydrogen system supplying a telecommunications facility in a remote area. The objectives are to have an optimum number of PV panels while reducing the maintenance visits. The results show a reduction in PV panels with reduced visits.

2.5 Summary

Summary of the literature is given in Table 2.1.

Table 2.1: Literature review summary

Ref	Type	Solar	Application	Objectives	Results
Kumari and Geethanjali (2017)	Adaptive GA	PV	PV design parameter extraction	Current, resistance	Fits curve efficiently at different irradiation conditions
Cortés et al. (2018)	BGA, SGA	PV	Electricity and heating operating cost optimization	Optimal configuration of energy supply	SGA converged faster with better quality than BGA
Muhsen et al. (2015)	DE with Integrated Mutation	PV	Modelling of PV modules	Extract photocurrent, diode current and ideality factor, series and shunt resistance	Fast convergence with reasonable accuracy with DEIM
Bucking and Dermardiros (2018)	Distributed EA	PV	Integrate building design with the energy system	Quantifies a building achieves a renewable energy balance	Integrated optimization scalable for future planning studies
Muhsen et al. (2016)	EA	PV	PV module single-diode parameter extraction	PV currents	Good accuracy, fewer control settings and fast convergence

Bastidas-Rodriguez et al. (2017)	GA	PV	PV module single-diode identification	Experimental I –V curves	η, Rs and Rh vary according to the weather conditions
Carotenuto et al. (2015)	EA	PV	Maximum power produced at the actual irradiance conditions	Optimize output power	Minimize computation time
Blaifi et al. (2016)	GA	PV	Dynamic battery model for PV	Battery voltage	Lower errors between predicted and real model
Youssef et al. (2016)	GA	PV	Net energy cost reduction for building	The dimension of the building, ratios in the building, the location of PV	Optimum design for BIPV from energy and cost
Shirzadi et al. (2014)	GA	PV	Minimizes mismatch losses more effectively	Optimum placement of modules in the array	Calculation of energy yield supports best yield arrangement
Rong et al. (2015)	hybrid GA	PV	Identification method for the PV parameter	Improve identification accuracy for those results with more substantial error	Identification results by the method are accurate
Daraban et al. (2014)	Modified GA	PV	Tracking MPP in PV	Input voltage	Algorithm optimizes with a good final solution
Siddiqui and Abido (2013)	Tabu Search + DE	PV	Predict PV electrical performance	Power-voltage curve, short circuit, open circuit and MPP	Tabu Search gives the lowest values of the objective function and most accurate
Singh et al. (2015b)	GA	PVT	PVT system efficiency improvement	Overall exergy and thermal efficiency	Overall efficiency increase for efficiency and exergy

Singh and Agrawal (2015)	GA–Fuzzy System	PVT	PVT system design parameters optimization	Overall exergy efficiency	GA–FS converges faster and solves better than GA
Singh and Agrawal (2016)	Fuzzified GA	PVT	Efficiency maximization and performance evaluation PV	Overall exergy efficiency	Electrical efficiency improved and optimized with reduced cell temperature
Singh et al. (2015)	EA	PVT	Glazed PVT array optimization	Overall exergy efficiency	Overall efficiency increase for thermal and exergy
Arias-Rosales and Mejía-Gutiérrez (2018)	GA-Weibull Arias	CPV	Solar harvest area increase	Material cost, effective concentration, space required	Efficient in finding solar V-Throughs setup
Burhan et al. (2016)	Micro GA	CPV	Convert irradiance to electricity for Hydrogen/ Oxygen gas	The optimum configuration of CPV-Hydrogen system	Reduce system cost with optimal storage factor
Jiménez-Fernández et al. (2014)	EA	hybrid PV	Optimize power system for a remote telecommunications facility	The optimum number of PV panels and number of maintenance visits	Reduction in the number of PV panels for unattended work of the system between two maintenance visits
Paulitschke et al. (2017)	GA	hybrid PV	Optimize energy for household using PV and fuel cell	Amount of power	Combine battery with a fuel cell to prolong life

CHAPTER 3

METHODOLOGY

To analyse the Power Conversion Efficiency (PCE) of solar PV modules for different locations, a detailed methodology based on experimental results and GA was devised. The study is essential in understanding how different locations can affect the PCE of different solar PV modules. The overall flowchart is shown in Figure 3.1.

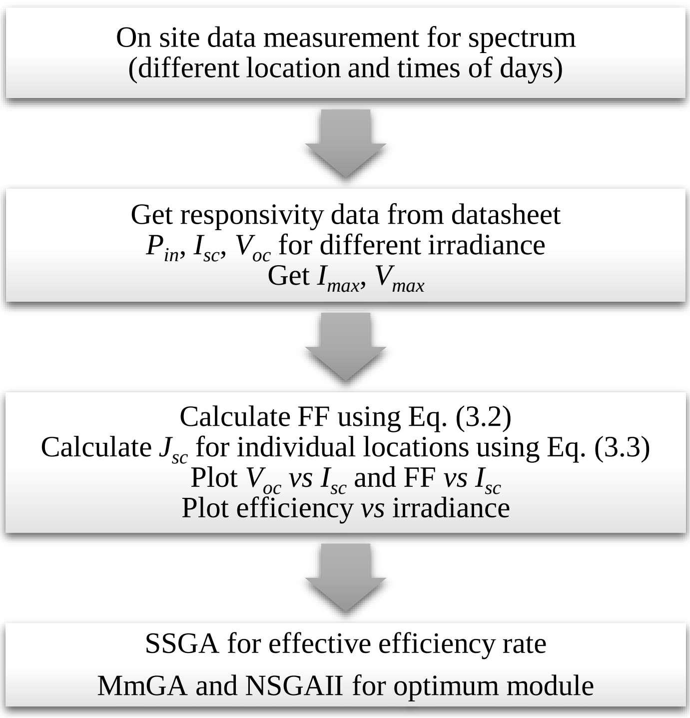

Figure 3.1: Overall flowchart

The first step is to take spectrum measurements at various locations, as shown in Table 3.1. The spectrum is measured during different times of the day. Next, data sheets from various manufacturers are downloaded and the responsivity data, Eq. (3.4) is taken. In addition, the P_{in}, I_{sc}, V_{oc} are noted from the datasheet and the I_{max} and V_{max} are then calculated.

Then, the fill factor (FF) is calculated using Eq. (3.2). The current density of a solar cell is calculated using Eq. (3.3). Open circuit voltage is plotted *vs* short-circuit current in Figure 3.5, and FF *vs* short-circuit current in Figure 3.6. Efficiency vs spectral irradiance is then plotted. Finally, SSGA is used in calculating the effective efficiency rates, while MmGA and NSGAII is used in selecting the optimum module.

3.1 Solar spectrum acquisition

To study the effect of local solar irradiance in a tropical country as compared to AM1.5G standard spectral irradiance, five locations in Peninsular Malaysia were chosen, as listed in Table 3.1.

Table 3.1: GPS coordinates of various locations

Location	GPS Coordinates
Sg Long, Selangor	3°04'08.0"N 101°79'42.0"E
Setapak, Kuala Lumpur	3°12'59.5"N 101°44'00.2"E
Bangi, Selangor	2°92'72.5"N 101°78'25.9"E
Bayan Lepas, Penang	5°20'07.5"N 100°18'05.8"E
Jitra, Kedah	6°15'28.1"N 100°25'12.2"E

For acquiring the full solar spectrum to cover the wavelengths ranging from 300 nm to 1800 nm, configuration of combined two types Avantes spectrometers comprised of AvaSpec-2048-USB2-RM (visible bandwidth 200–1100 nm) and AvaSpec-NIR256-1.7-RM (infrared bandwidth 1000–2000 nm), as shown in Figure 3.2 were used. The data is captured using AvaSoft, as shown in Figure 3.3. For data acquisition, a mostly sunny day in the month of October 2017 was selected to assess how the solar spectrum varies across the day.

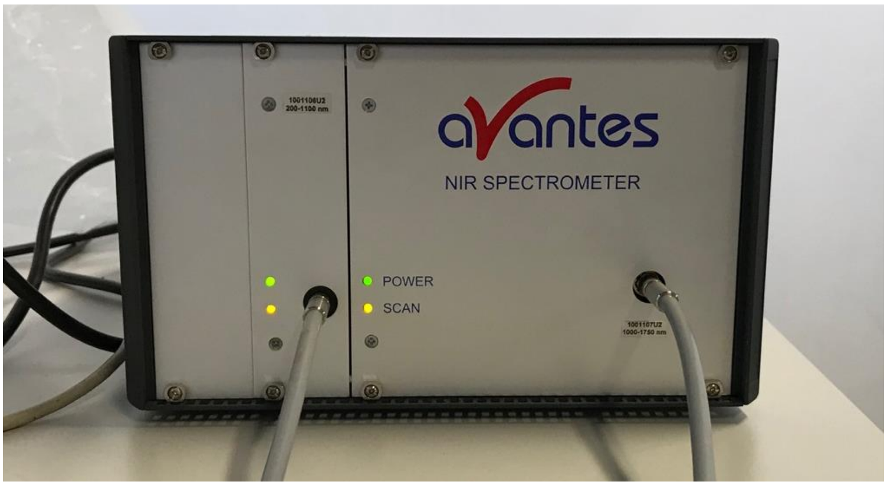

Figure 3.2: Avantes NIR Spectrometer

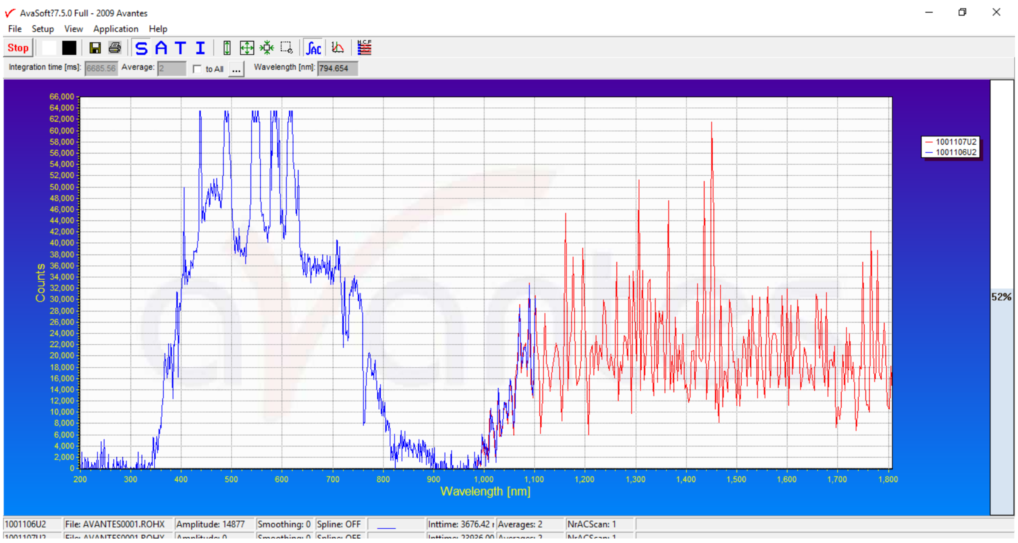

Figure 3.3: AvaSoft software

While there were numerous readings taken during the day, the maximum recorded irradiance during the day are as follows: Sg Long 832.46 W/m^2, Setapak 876.21 W/m^2, Bangi 802.74 W/m^2, Bayan Lepas 808.35 W/m^2, and Jitra 706.80 W/m^2. The spectral irradiance versus the wavelength for different locations ranging from 300 to 1700 nm is shown in Figure 3.4. It can be seen that the values at each wavelength are different at different locations, with some locations overlapping at specific wavelengths. This creates the difference in the output of the PV solar module.

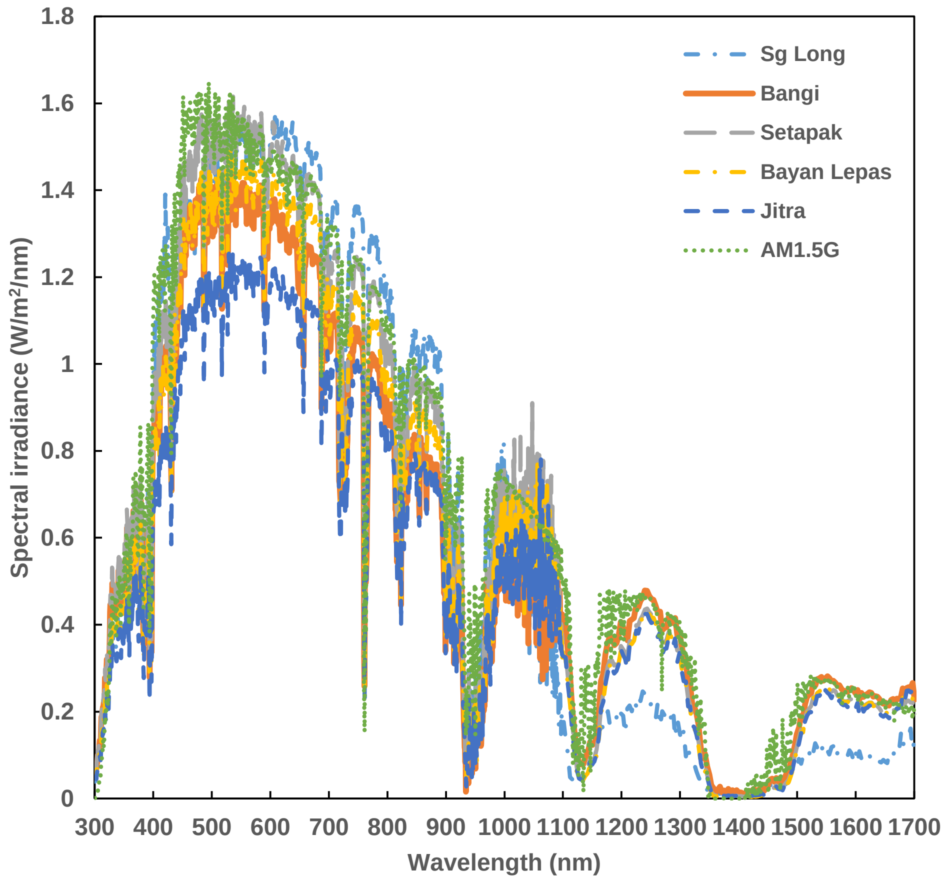

Figure 3.4: Spectral irradiance of the local spectrum at different locations

3.2 Solar irradiance

To analyse the Power Conversion Efficiency (PCE) of solar cells under different spectral irradiances, a detailed methodology based on experimental results and a computational algorithm is formulated. PCE can be calculated using

$$\mathrm{PCE} = \frac{FF \times J_{sc}V_{oc}}{P_{in}/A} \tag{3.1}$$

where J_{max} (mA/cm^2) and V_{max} (V) are the current density and voltage at the maximum power point, respectively; P_{in}/A is the incident light intensity with unit mW/cm^2 in which P_{in} is a power of incident light in unit mW, and A is the corresponding area (cm^2).

The study is essential to understand the PCE for various types of photovoltaic devices, and here demonstrated for solar cells, under different spectral irradiances.

In the proposed methodology, the first step is to obtain the electrical characteristics of solar cells from the datasheet. The External Quantum Efficiency (EQE), input power P_{in}, short-circuit current I_{sc}, open-circuit voltage V_{oc}, maximum current I_{max}, and maximum voltage V_{max} is first taken from the various manufacturer datasheets. Then, the Fill Factor (FF) is calculated using

$$\mathrm{FF} = \frac{J_{max} V_{max}}{J_{sc} V_{oc}} \tag{3.2}$$

The current density of a solar cell can be calculated using the following equation:

$$J_{sc} = \int_{\lambda_1}^{\lambda_2} S_L(\lambda) \cdot R(\lambda)\, \mathrm{d}\lambda \tag{3.3}$$

λ_1 and λ_2 are the lower limit and upper limit wavelengths of incident light respectively, $S_L(\lambda)$ is spectral irradiance of local spectrum. $R(\lambda)$ is the spectral responsivity of the device, given as

$$R(\lambda) = \frac{e\lambda}{hc} \eta_{EQE}(\lambda) \tag{3.4}$$

where η_{EQE} is the external quantum efficiency of the device, λ is the wavelength of incidence light, h is Planck's constant, c is the speed of light.

Incident light intensity can be calculated as

$$\frac{P_{in}}{A} = \int_{\lambda_1}^{\lambda_2} S_L(\lambda) \mathrm{d}\lambda \tag{3.5}$$

3.3 Specifications

Specifications of the various solar modules are listed in Table 3.2. A total of twelve types of modules from eleven manufacturers are used. The material used ranges from monocrystalline silicon to polycrystalline silicon. Some of the cells are a combination of multiple materials. The PCEs of various commercial PV modules are obtained from the datasheet ranging from 7.1% to 21.2% based on the AM1.5G rated values.

Table 3.2: Specifications of solar modules

<table>
<tr><th>Type</th><th>Manufacturer</th><th>Model</th><th>Material</th><th>PCE AM1.5G</th></tr>
<tr><td>1</td><td>SunPower</td><td>SPR-X21-345</td><td rowspan="2">Monocrystalline Silicon</td><td>21.167%</td></tr>
<tr><td>2</td><td>Wattrom</td><td>WT 255M17</td><td>16.391%</td></tr>
<tr><td>3</td><td>Sanyo</td><td>HIT-H250E01</td><td>Monocrystalline Silicon + Amorphous Silicon</td><td>18.077%</td></tr>
<tr><td>4</td><td>DelSolar</td><td>D6P250B3A</td><td rowspan="2">Multicrystalline Silicon</td><td>15.385%</td></tr>
<tr><td>5</td><td>SunPower</td><td>SPR-P17-350-COM</td><td>16.965%</td></tr>
<tr><td>6</td><td>Hanwha Q CELLS</td><td>Q.PLUS L-G4.2 340</td><td rowspan="4">Polycrystalline Silicon</td><td>17.041%</td></tr>
<tr><td>7</td><td>IndoSolar</td><td>ISLM-270</td><td>16.838%</td></tr>
<tr><td>8</td><td>SolarWorld</td><td>Sunmodule SW 260</td><td>15.675%</td></tr>
<tr><td>9</td><td>Sunbe Solar</td><td>SPM(P)255</td><td>14.969%</td></tr>
<tr><td>10</td><td>Schott</td><td>ASI 103</td><td>Amorphous Silicon</td><td>7.116%</td></tr>
<tr><td>11</td><td rowspan="2">First Solar</td><td>FS-387</td><td>CdS/CdTe Silicon</td><td>12.163%</td></tr>
<tr><td>12</td><td>FS-4117-2</td><td>CdTe Silicon</td><td>16.317%</td></tr>
</table>

Based on data provided by Sustainable Energy Development Authority (SEDA, 2017) Malaysia, the annual solar radiation for different locations is listed in Table 3.3. The highest annual radiation is at Bayan Lepas, Penang, a city located in the northern region of Peninsular Malaysia, whilst the lowest recorded value is at Bangi, Selangor.

Table 3.3: Annual solar radiation (SEDA, 2017)

Location	**kWh/m²**
Sg Long, Selangor	1572
Setapak, Kuala Lumpur	1571
Bangi, Selangor	1487
Bayan Lepas, Penang	1809
Jitra, Kedah	1750

3.4 Case study at Sg Long

There are many combinations of locations and types of PV modules in this study. To show the detailed procedure in the methodology, only one of the locations is selected, i.e., Sg Long with module type 4 from Delsolar as a sample case study. The first relationship between V_{oc} and J_{sc} is investigated by extracting values under different irradiances, as shown in Figure 3.5. The empirical formula is

$$Voc = 1.9821\, ln(Jsc) + 32.976 \tag{3.6}$$

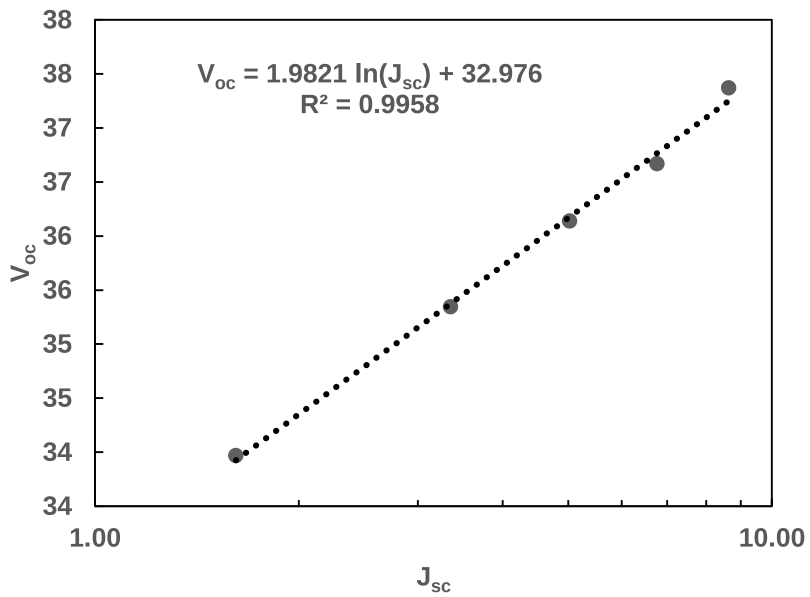

Figure 3.5: The relationship between open circuit voltage (V_{oc}) and short-circuit current density (J_{sc}) of solar cells under different irradiances

The relationship between FF and J_{sc} under different irradiances is shown in Figure 3.6. Based on the observations in Chong et al. (2016), the FF vs J_{sc} curve should behave as a logarithmic function.

$$FF = -0.025\, ln(Jsc) + 0.8451 \tag{3.7}$$

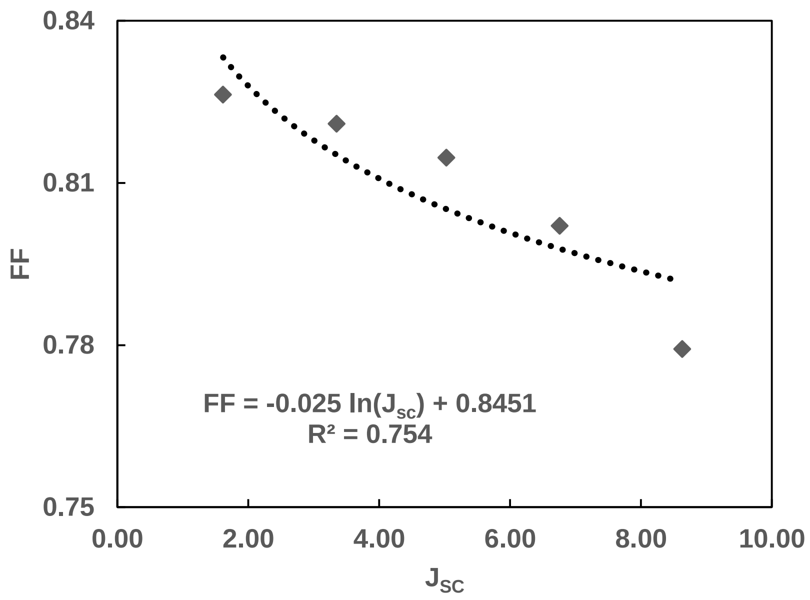

Figure 3.6: The relationship between fill factor (FF) and short circuit current density (J_{sc}) of solar cells under different irradiances

Responsitivity of the module type 4 is shown in Figure 3.7. It can be seen that the graph slowly increases to the peak value of 960 nm and then it descends quickly.

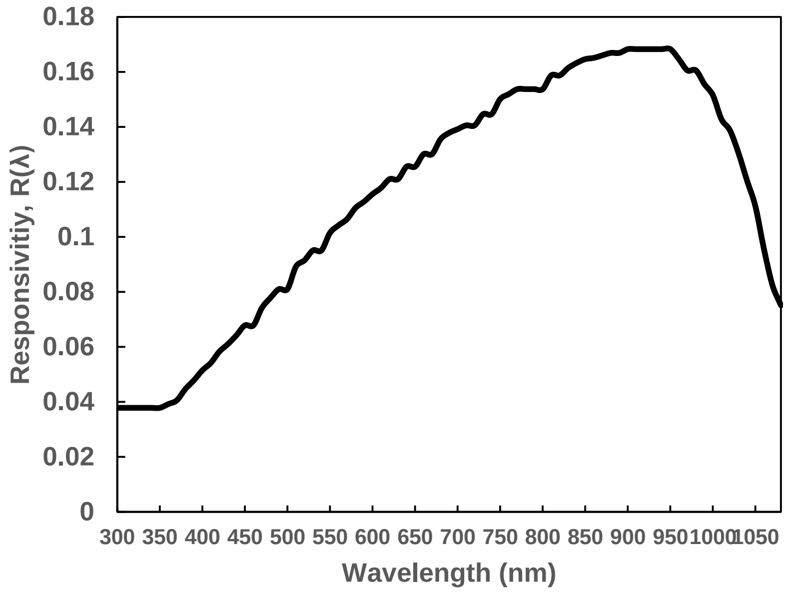

Figure 3.7: The responsivity of the solar cell at various wavelengths

As it is not possible to get the irradiance by increments of 100 W/m^2, five readings throughout the day were taken. The efficiency vs irradiance is plotted for location Sg Long using solar module type 4 in Figure 3.8. The empirical formula of FF versus J_{sc} plot can be expressed by the following equation:

$$Eff = 0.0036\, ln(Irr) + 0.1267 \tag{3.8}$$

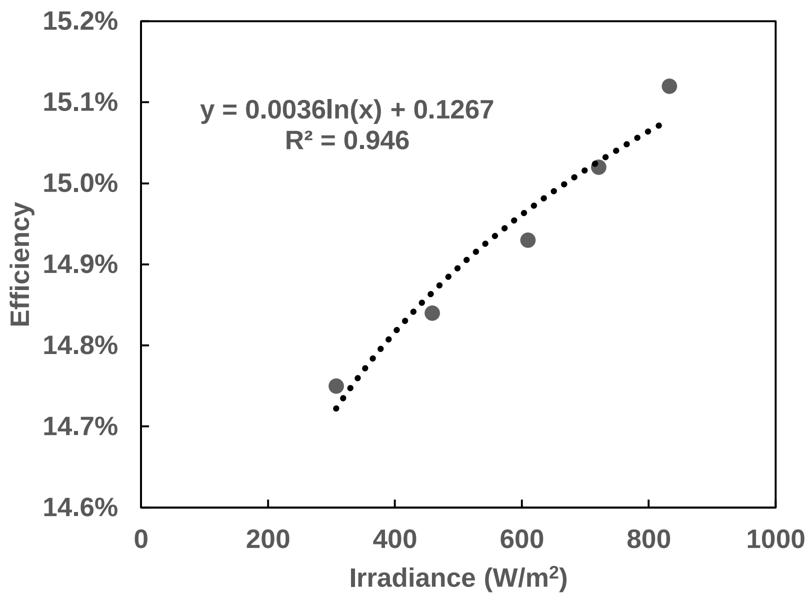

Figure 3.8: The relationship of efficiency under different irradiances

3.5 Genetic Algorithm

Genetic Algorithm (GA) (Holland, 1992) is a class of the Evolutionary Algorithm (EA). Borrowing the idea of natural selection and learning process, EA establishes an effective computing system for problem-solving (Tan et al., 2013). The search progresses in parallel by maintaining a pool of candidate solutions; each known as a chromosome in the context of GA. In turn, an individual is associated with a fitness value, which is evaluated through a problem-specific objective function. The fitness value determines the quality of the individual. Fitter individuals are often preferred by GA. The population evolves (iterates) through repeated applications of various operations, such as selection, mutation and crossover until some predefined termination conditions are satisfied. Each iteration step is referred to as a generation.

GAs have been used from simple to complex engineering problems. In the following sub-sections, the details of three GA variants are given.

3.5.1 Steady State Genetic Algorithm

Steady State Genetic Algorithm (SSGA) is a GA variant (Vavak & Fogarty, 1996; Agapie & Wright, 2014). The GA is in a steady state, where there are no generations. As compared to the generic GA, the tournament selection does not replace the individuals in the population. Instead, in SSGA, two best individuals are added to the population to ensure the population size remains constant.

The algorithm is given in Algorithm 3.1, where heuristic functions G and D_r both depend on x, the current population. As such, i is selected from the probability distribution $G(x)$, and j is selected from the probability distribution $D_r(x)$. Let Ω denote the search space for a search problem.

1. Choose an initial population η of size r.
2. $x \leftarrow \eta$.
3. Select i from Ω using the probability distribution $\mathcal{G}(x)$.
4. Select j using the probability distribution $\mathcal{D}_r(x)$.
5. Replace x by $x - e_j/r + e_i/r$.
6. Go to step 3.

Algorithm 3.1: SSGA algorithm (Agapie & Wright, 2014)

Random deletion can be modelled by choosing $D_r(x) = x$. If the fitness function is injective (the fitnesses of elements are distinct), then reverse ranking, and worst-element deletion can be modelled using the framework developed for ranking selection,

$$D_r(x)_i = \int_{\Sigma_{\{j:f_j<f_i\}} x_j}^{\Sigma_{\{j:f_j\ll f_i\}} x_j} \varrho(s)ds \tag{3.9}$$

The probability density function $\varrho(s)$ can be chosen to be $2s$ to model standard ranking selection, and $2 - 2s$ to model reverse ranking deletion. If D_r is iterated, after the first iteration the populations produced will not necessarily correspond to finite populations of size r. For random deletion and reverse ranking deletion, $D_r(x)$ does not depend on the population size and can be shown to be differentiable as a function of x.

3.5.2 Non-dominated Sorting Genetic Algorithm II

Non-dominated Sorting Genetic Algorithm II (NSGAII) is designed with objectives of overcomes limitations in NSGA, which has high computational complexity of non-dominated sorting (Deb et al., 2002). Specifically, a fast non-dominated sorting approach with $O(MN^2)$ computational complexity is presented. Also, a selection operator is presented that creates a mating pool by combining the parent and offspring populations and selecting the best (with respect to fitness and spread) solutions.

NSGAII has good experimental results in terms of the spread of solutions as well as better convergence (near the true Pareto-optimal) measurements. The step-by-step procedure (Figure 3.9) shows that NSGAII algorithm is simple and straightforward. First, a combined population $R_t = P_t \cup Q_t$ is formed. The population is of size R_t. Then, the population R_t is sorted according to non-domination. Since all previous and current population members are included in, elitism is ensured. Now, solutions belonging to the best non-dominated set F_1 are of best solutions in the combined population and must be emphasized more than any other solution in the combined population. If the size of F_1 is smaller than N, all members of the set F_1 are chosen for the new population P_{t+1}. The remaining members of the population P_{t+1} are chosen from subsequent non-dominated fronts in the order of their ranking. Thus, solutions from the set F_2 are chosen next, followed by solutions from the set F_3, and so on. This procedure is continued until no more sets can be accommodated.

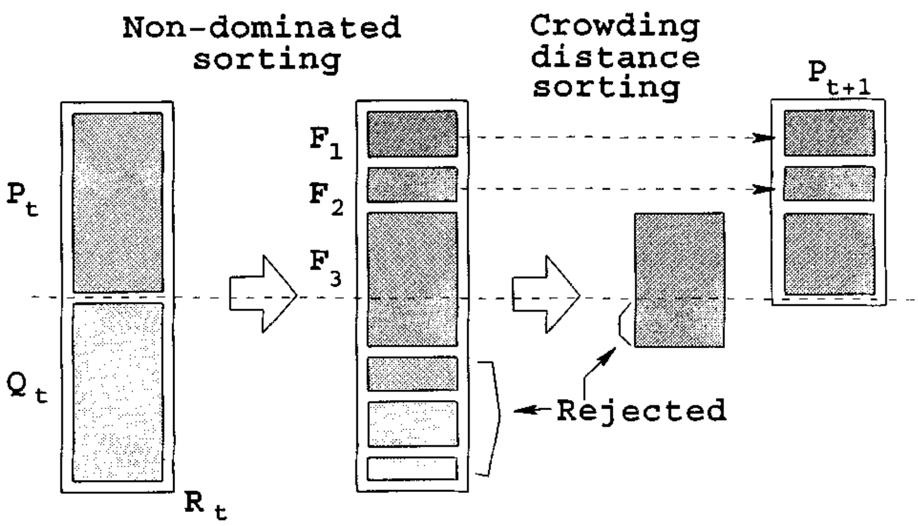

Figure 3.9: NSGAII procedure (Deb et al., 2002)

The NSGAII procedure is also shown in Algorithm 3.2. The new population P_{t+1} of size N is now used for selection, crossover, and mutation to create a new population Q_{t+1} of size N. The fast non-dominated sorting (FNDS) of NSGAII requires $O(MN^2)$ time computations. All solutions in the first non-dominated front will have their, domination count as zero. Now, for each solution p with $n_p = 0$, each member (q) of its set S_p is visited and reduce its domination count by one. In doing so, if for any member q the domination count becomes zero, it is put in a separate list *Q*. These members belong to the second non-dominated front. Now, the above procedure is continued with each member of *Q*, and the third front is identified. This process continues until all fronts are identified and locate the FDNS using Algorithm 3.2.

`fast-non-dominated-sort`(P)	
for each $p \in P$	
$S_p = \emptyset$	
$n_p = 0$	
for each $q \in P$	
if $(p \prec q)$ then	If p dominates q
$S_p = S_p \cup \{q\}$	Add q to the set of solutions dominated by p
else if $(q \prec p)$ then	
$n_p = n_p + 1$	Increment the domination counter of p
if $n_p = 0$ then	p belongs to the first front
$p_{\text{rank}} = 1$	
$\mathcal{F}_1 = \mathcal{F}_1 \cup \{p\}$	
$i = 1$	Initialize the front counter
while $\mathcal{F}_i \neq \emptyset$	
$Q = \emptyset$	Used to store the members of the next front
for each $p \in \mathcal{F}_i$	
for each $q \in S_p$	
$n_q = n_q - 1$	
if $n_q = 0$ then	q belongs to the next front
$q_{\text{rank}} = i + 1$	
$Q = Q \cup \{q\}$	
$i = i + 1$	
$\mathcal{F}_i = Q$	

Algorithm 3.2: Fast-non-dominated-sort in NSGAII (Deb et al., 2002)

3.5.3 Modified micro Genetic Algorithm

The modified micro Genetic Algorithm (MmGA) was proposed in Tan et al. (2013). MmGA is formed with three objectives:

1. Originality: to preserve the traditional mGA (Coello & Pulido, 2001; 2005) principles in the proposed MmGA. An NSGAII inspired elitism strategy is adopted in its algorithm formation.
2. Efficiency: to achieve improvement in convergence representation as indicated by Generational Distance (GD) (Deb et al., 2002; Coello & Pulido, 2005) indicator. GD is used for measuring the distance between the computed approximation and the optimal Pareto front. The computed

approximation is claimed to locate on the right Pareto front as value GD = 0.

3. Simplicity: to preserve the complexity of the proposed model as compared with NSGAII. MmGA has the same time complexity as NSGAII, i.e. $O(MN^2)$, where M is the number of objectives and N is the population size.

Original mGA is adapted for the formation of MmGA, as shown in Algorithm 3.3. mGA was formulated based on the GA principles (Goldberg, 1989), but with small population size. It usually contains only three to six chromosomes in its population. On the other hands, MmGA covers three main components as follows.

An NSGAII inspired elitism strategy is incorporated into the mGA. In the elitism method, a user-defined elite-preservation size (ω) of selected chromosomes (x) and target chromosomes (y) are derived. The elitism method produces *a* vector z as its outcome, which consists of ω-elite chromosomes. Note that x and y are the vectors of chromosomes, which exist in the evolutionary and filter processes within both nominal and outlier evolution cycles, respectively.

The second component is an extended population formation. The population of chromosomes is re-initialised (p) using four main components in MmGA. An adapting of the Pareto dominance sorting concept with the above two methods is the last main component of MmGA. It has the aim of improving the converged solutions, as measured by GD.

```
Procedure MmGA    ▷ O(MN^2)
i = 0, p_MmGA = φ
em = f(archiveSize, BiSection, n) = φ
Initialise m_init
*m = Sort(m_init, ⪯)    ▷ O(N)
while i < evaluation_Max do    ▷ O(c0)
    *p_init = InitialisePopulation(n, ratio, irm,
rm, m)    ▷ O(c0 × N^2)
    *p = Sort(p_init, ⪯)    ▷ O(c0 × N)
    repeat
        u = Binary tournament selection on p
        v = Two-Point crossover on u
        w = Uniform mutation on v
        p_MmGA_i = *MmGAElitism(w, p, 1)
  ▷ O(c0 × c1 × MN^2)
        Produce the next generation
    until  nominalConvergence_Max  is  reached
▷ O(c1)
    em_MmGA = *^1 MmGAElitism(p_MmGA_i,
em, eliteSize)    ▷ O(c0 × MN^2)
    if em is full when trying to insert em_elite then
        em = adaptiveGrid(em_elite) [50]
  ▷ O(eliteSize × c0 × N)
    end if
    m = *^2 MmGAElitism(p_MmGA_i, m, eliteSize)
  ▷ O(c0 × MN^2)
    if i modulus replacementCycle then
        rm = *^3 MmGAElitism(em, rm, eliteSize)
  ▷ O(c0 × MN^2)
    end if
    i = i + 1
end while
return p_MmGA
  ▷ * the modification compare to previous works
[13, 16, 55, 56]
  ▷ *^1, *^2, *^3 are first, second and third form of
elitism mGA [13, 16] respectively
```

Algorithm 3.3: MmGA algorithm (Tan et al., 2013)

3.5.4 Experimental setup

The first part of the experiments utilize SSGA. The aim of using SSGA is to acquire effective PCE rate at an irradiance of 100 to 1000 W/m^2 with an increment of 100 W/m^2. Experimental of SSGA was conducted with a set of parameters as in Table 3.4.

Table 3.4: SSGA settings

Settings	**Value**
Population size	100 chromosomes
Max. evolution	25000 cycles
Crossover operator	Simulated Binary Crossover (SBX) with probability rate 0.9 and distribution index 20
Mutation operator	Polynomial Mutation Operator with probability rate 1.0 and distribution index 20
Selection operator	Binary Tournament Selection
Decision variable	Spectrum range from 100 to 1000
Objective variable	PCE

The second part of the experiments utilize both MmGA and NSGAII. Previous work published the capability of MmGA in tackling the benchmark Kursawe equation (Tan et al., 2013) and real-world MOPs (Tan et al., 2015), with small population size. Observation shows that MmGA gives statistical similar and better-optimized values in handling the real-world problem with a small population. Experiments are conducted with a similar set of settings, except the population size for MmGA, as shown in Table 3.5.

Table 3.5: MmGA and NSGAII settings

Settings	**MmGA**	**NSGAII**
Crossover operator	SBX crossover	SBX crossover
Probability rate	0.6	0.6
Distribution Index	20.0	20.0
Mutation operator	Polynomial mutation	Polynomial mutation
Probability rate	1.0	1.0
Distribution Index	20.0	20.0
Selection operator	Binary tournament	Binary tournament
Population size	4	100
Max evaluation cycle	10000	10000

To signify the all results statistically from the GA variants, the bootstrap method (Efron & Tibshirani, 1993) was utilized. Typically, a thousand bootstrapped samples provide useful estimates, while doubling that amount provide useful results (Efron & Tibshirani, 1993). The performance metrics in this study were calculated using a million samples that were bootstrapped with 95% confidence intervals to give accurate estimated results.

CHAPTER 4

RESULTS AND DISCUSSION

4.1 Results using SSGA

To view the effect of solar radiance on the PCE, the rates calculated using SSGA. Results are shown in Tables 4.1 to 4.5. Intervals of 100 W/m^2 are used as it gives a representation of the entire spectrum, with graphs typically plotted in this scale (Muneer, 2007). In general, it can be seen that the minimum and maximum PCE values are stable, with a slight variance in between.

The efficiencies at Sg Long is first taken into account in Table 4.1. It can be seen that module type 10 has the lowest efficiencies and the PCE is stable throughout the different irradiance. Module type 12 has the most significant variance in PCE, with a difference of 7.7% from the lowest to the highest point. Most other modules have an average difference of 2% to 3%, with the peak of 1000 W/m^2 having the best PCE.

Table 4.1: Efficiencies by solar radiance (W/m^2) at Sg Long

Type	100	200	300	400	500	600	700	800	900	1000
1	11.1%	11.6%	12.2%	12.8%	13.4%	14.0%	14.6%	15.2%	15.8%	16.4%
2	13.3%	13.7%	14.1%	14.4%	14.8%	15.2%	15.6%	16.0%	16.4%	16.8%
3	15.6%	15.9%	16.1%	16.4%	16.6%	16.9%	17.1%	17.4%	17.6%	17.9%
4	13.5%	13.7%	14.0%	14.3%	14.6%	14.8%	15.1%	15.4%	15.7%	16.0%
5	12.6%	13.2%	13.8%	14.4%	15.0%	15.6%	16.2%	16.8%	17.4%	18.0%
6	13.4%	13.9%	14.4%	14.8%	15.3%	15.8%	16.2%	16.7%	17.2%	17.6%
7	13.2%	13.7%	14.2%	14.7%	15.2%	15.7%	16.2%	16.7%	17.2%	17.7%
8	13.0%	13.4%	13.7%	14.1%	14.4%	14.8%	15.2%	15.5%	15.9%	16.2%
9	12.5%	12.8%	13.1%	13.3%	13.6%	13.9%	14.2%	14.5%	14.8%	15.1%
10	7.9%	7.9%	7.8%	7.8%	7.8%	7.7%	7.7%	7.6%	7.6%	7.6%
11	8.6%	9.3%	9.9%	10.5%	11.1%	11.7%	12.4%	13.0%	13.6%	14.2%
12	11.2%	12.1%	12.9%	13.8%	14.6%	15.5%	16.3%	17.2%	18.1%	18.9%

Next, efficiencies at Setapak is listed in Table 4.2. Module type 7 has the most significant difference from the lowest to highest, at 4.4%, while the other module difference is about 2% to 3%.

Table 4.2: Efficiencies by solar radiance (W/m^2) at Setapak

Type	100	200	300	400	500	600	700	800	900	1000
1	12.7%	12.9%	13.1%	13.4%	13.6%	13.8%	14.0%	14.2%	14.4%	14.6%
2	12.7%	12.9%	13.2%	13.5%	13.8%	14.1%	14.4%	14.7%	14.9%	15.2%
3	13.1%	13.5%	13.9%	14.3%	14.7%	15.0%	15.4%	15.8%	16.2%	16.6%
4	12.5%	12.7%	12.9%	13.1%	13.3%	13.5%	13.7%	14.0%	14.2%	14.4%
5	13.7%	14.0%	14.2%	14.5%	14.7%	15.0%	15.3%	15.5%	15.8%	16.0%
6	13.0%	13.3%	13.6%	14.0%	14.3%	14.6%	14.9%	15.2%	15.6%	15.9%
7	11.6%	12.1%	12.6%	13.1%	13.6%	14.1%	14.6%	15.0%	15.5%	16.0%
8	13.0%	13.2%	13.4%	13.6%	13.8%	14.0%	14.2%	14.4%	14.6%	14.8%
9	11.2%	11.5%	11.8%	12.1%	12.3%	12.6%	12.9%	13.1%	13.4%	13.7%
10	7.6%	7.6%	7.6%	7.5%	7.5%	7.4%	7.4%	7.3%	7.3%	7.2%
11	11.3%	11.4%	11.4%	11.5%	11.6%	11.6%	11.7%	11.7%	11.8%	11.9%
12	15.0%	15.1%	15.3%	15.4%	15.5%	15.6%	15.7%	15.8%	15.9%	16.0%

For the efficiencies at Bangi, module type 4 has the most significant difference from the lowest to highest, at 2.2%, as listed in Table 4.3. The difference in most other modules are small, at about 1% or less.

Table 4.3: Efficiencies by solar radiance (W/m^2) at Bangi

Type	**100**	**200**	**300**	**400**	**500**	**600**	**700**	**800**	**900**	**1000**
1	13.6%	13.7%	13.7%	13.8%	13.8%	13.9%	13.9%	13.9%	14.0%	14.0%
2	14.0%	14.0%	14.1%	14.1%	14.2%	14.2%	14.2%	14.3%	14.3%	14.3%
3	14.9%	15.0%	15.0%	15.1%	15.1%	15.1%	15.2%	15.2%	15.3%	15.3%
4	11.7%	12.0%	12.2%	12.5%	12.7%	13.0%	13.3%	13.5%	13.8%	14.0%
5	14.7%	14.8%	14.9%	15.0%	15.1%	15.1%	15.2%	15.3%	15.4%	15.4%
6	14.4%	14.5%	14.5%	14.6%	14.7%	14.7%	14.8%	14.9%	14.9%	15.0%
7	13.4%	13.6%	13.7%	13.9%	14.1%	14.3%	14.5%	14.6%	14.8%	15.0%
8	14.0%	14.0%	14.1%	14.1%	14.1%	14.1%	14.1%	14.1%	14.1%	14.1%
9	12.6%	12.6%	12.6%	12.7%	12.7%	12.7%	12.8%	12.8%	12.8%	12.9%
10	7.4%	7.3%	7.3%	7.3%	7.2%	7.2%	7.2%	7.2%	7.1%	7.1%
11	11.0%	11.1%	11.1%	11.2%	11.3%	11.4%	11.4%	11.5%	11.6%	11.7%
12	15.2%	15.2%	15.3%	15.3%	15.4%	15.4%	15.4%	15.5%	15.5%	15.6%

Next, PCE at Bayan Lepas is looked into in Table 4.4. Module type 10 exhibits similar results. The module with the most significant variance, however, is type 1, with a difference of 2.2%. The difference between the lowest and highest PCE for most modules is lower as compared to Sg Long, at around 1%.

Table 4.4: Efficiencies by solar radiance (W/m^2) at Bayan Lepas

Type	**100**	**200**	**300**	**400**	**500**	**600**	**700**	**800**	**900**	**1000**
1	12.5%	12.7%	13.0%	13.2%	13.5%	13.7%	14.0%	14.2%	14.5%	14.7%
2	13.8%	14.0%	14.1%	14.2%	14.4%	14.5%	14.7%	14.8%	14.9%	15.1%
3	15.5%	15.6%	15.6%	15.7%	15.8%	15.9%	16.0%	16.1%	16.1%	16.2%
4	14.0%	14.0%	14.0%	14.0%	14.1%	14.1%	14.1%	14.1%	14.2%	14.2%
5	14.0%	14.2%	14.4%	14.7%	14.9%	15.1%	15.4%	15.6%	15.8%	16.1%
6	14.3%	14.5%	14.6%	14.8%	14.9%	15.1%	15.2%	15.4%	15.5%	15.7%
7	14.3%	14.4%	14.6%	14.7%	14.9%	15.0%	15.1%	15.3%	15.4%	15.6%
8	13.5%	13.6%	13.8%	13.9%	14.1%	14.2%	14.3%	14.5%	14.6%	14.8%
9	12.8%	12.9%	13.0%	13.0%	13.1%	13.2%	13.3%	13.3%	13.4%	13.5%
10	7.3%	7.3%	7.3%	7.3%	7.3%	7.3%	7.3%	7.3%	7.3%	7.3%
11	11.6%	11.6%	11.6%	11.7%	11.7%	11.7%	11.8%	11.8%	11.8%	11.9%
12	14.8%	15.0%	15.1%	15.2%	15.4%	15.5%	15.6%	15.7%	15.9%	16.0%

For the efficiencies at Jitra, module type 7 has the most significant difference from the lowest to highest, at 3.6%, as listed in Table 4.5. The difference in most other modules are about 2% to 3%.

Table 4.5: Efficiencies by solar radiance (W/m^2) at Jitra

Type	100	200	300	400	500	600	700	800	900	1000
1	12.8%	13.0%	13.1%	13.3%	13.5%	13.7%	13.9%	14.0%	14.2%	14.4%
2	13.1%	13.3%	13.5%	13.7%	14.0%	14.2%	14.4%	14.7%	14.9%	15.1%
3	13.6%	13.9%	14.3%	14.6%	14.9%	15.3%	15.6%	16.0%	16.3%	16.7%
4	12.9%	13.1%	13.2%	13.4%	13.5%	13.7%	13.8%	14.0%	14.1%	14.3%
5	14.0%	14.2%	14.4%	14.6%	14.8%	15.0%	15.2%	15.4%	15.6%	15.8%
6	13.5%	13.8%	14.0%	14.3%	14.5%	14.7%	15.0%	15.2%	15.5%	15.7%
7	12.4%	12.8%	13.2%	13.6%	14.0%	14.4%	14.8%	15.2%	15.6%	16.0%
8	13.3%	13.4%	13.6%	13.7%	13.9%	14.0%	14.2%	14.4%	14.5%	14.7%
9	11.8%	12.0%	12.2%	12.4%	12.6%	12.8%	13.0%	13.2%	13.4%	13.6%
10	7.4%	7.4%	7.3%	7.3%	7.2%	7.2%	7.1%	7.0%	7.0%	6.9%
11	11.4%	11.4%	11.4%	11.4%	11.4%	11.4%	11.5%	11.5%	11.5%	11.5%
12	14.6%	14.7%	14.8%	14.9%	15.1%	15.2%	15.3%	15.4%	15.6%	15.7%

It can be seen that there is a variation of module PCE based on module type by location, and the different modules respond differently to the different irradiance levels, with some having smaller differences than the other. Selecting a panel with high PCE and small differences between different irradiances is essential in order to generate a stable output.

Table 4.6 lists the PCE, gain, and annual energy yield by location and solar module type. The minimum and maximum output for all modules are 106 and 341 kWh/m^2 per year, respectively. The highest value is recorded at Bayan Lepas using module type 1 (SunPower SPR-X21-345). The average value is 237 kWh/m^2 per year.

At the same time, a comparison of PCE for commercial PV modules under the local spectral irradiances relative to AM1.5G spectrum is done by defining the following new parameter:

$$Gain = 100\% \times \frac{(\mathrm{PCE_{LSI}} - \mathrm{PCE_{AM1.5G}})}{\mathrm{PCE_{AM1.5G}}} \tag{4.1}$$

where $\mathrm{PCE_{LSI}}$ and $\mathrm{PCE_{AM1.5G}}$ are the power-conversion efficiencies for local spectral irradiances and under AM1.5G conditions, respectively.

In terms of gain, the most stable module is module type 10, which also has the lowest PCE. The most significant gain loss is at Bangi using module type 3 with -15.8% difference with AM1.5G. The general gain loss is about 6%.

The annual energy yields, in kWh/m^2 is also given. It can be seen that the various modules at different locations all give different results. The PCE values fluctuate from each module at a different location.

Figure 4.1 shows the annual energy yields using modules 1 to 12 at the five locations. The chart is first separated by the 12 different types of modules, and for each module type, 5 locations are taken into account. At a glance, it can be seen that the highest energy yield for every single module comes from Bayan Lepas, mainly due to the amount of irradiance it receives. On the other hand, while Bangi has the least irradiance, the module outputs are not the lowest among all module types.

From the results, it can be seen and said that the amount of energy yield varies significantly by type of module and location. As such, selecting the right module at the specific location is vital to maximize the energy yield.

Table 4.6: PCE, gain, and annual energy yield by location and solar module type

Type	Sg Long			Setapak			Bangi			Bayan Lepas			Jitra		
	PCE	**Gain**	**kWh/m^2**	**PCE**	**Gain**	**kWh/m^2**	**PCE**	**Gain**	**kWh/m^2**	**PCE**	**Gain**	**kWh/m^2**	**PCE**	**Gain**	**kWh/m^2**
1	20.4%	-3.8%	320	19.1%	-9.7%	300	18.4%	-12.9%	274	18.9%	-10.9%	341	18.3%	-13.3%	321
2	16.1%	-1.5%	254	14.9%	-8.9%	235	14.3%	-13.0%	212	14.8%	-9.7%	268	14.5%	-11.8%	253
3	17.5%	-3.0%	276	16.1%	-10.7%	254	15.2%	-15.8%	226	16.1%	-11.1%	291	15.7%	-13.3%	274
4	15.5%	0.9%	244	14.2%	-7.8%	223	13.5%	-12.1%	201	14.1%	-8.2%	256	13.8%	-10.2%	242
5	16.8%	-1.0%	264	15.8%	-7.0%	248	15.3%	-9.9%	227	15.6%	-7.9%	283	15.2%	-10.2%	267
6	16.8%	-1.3%	264	15.5%	-8.9%	244	14.9%	-12.8%	221	15.4%	-9.7%	278	15.0%	-11.9%	263
7	16.9%	0.2%	265	15.5%	-8.2%	243	14.7%	-13.0%	218	15.3%	-9.0%	277	14.9%	-11.8%	260
8	15.6%	-0.5%	245	14.6%	-6.9%	229	14.1%	-10.1%	209	14.5%	-7.6%	262	14.2%	-9.4%	249
9	14.6%	-2.4%	230	13.4%	-10.5%	211	12.8%	-14.6%	190	13.3%	-11.0%	241	13.0%	-13.0%	228
10	7.6%	6.7%	119	7.3%	2.0%	114	7.1%	0.1%	106	7.3%	2.0%	131	7.0%	-1.1%	123
11	12.8%	5.1%	201	11.8%	-2.7%	186	11.5%	-5.3%	171	11.8%	-2.9%	214	11.5%	-5.8%	200
12	17.0%	4.1%	267	15.9%	-2.8%	249	15.5%	-5.1%	230	15.8%	-3.4%	285	15.3%	-6.1%	268

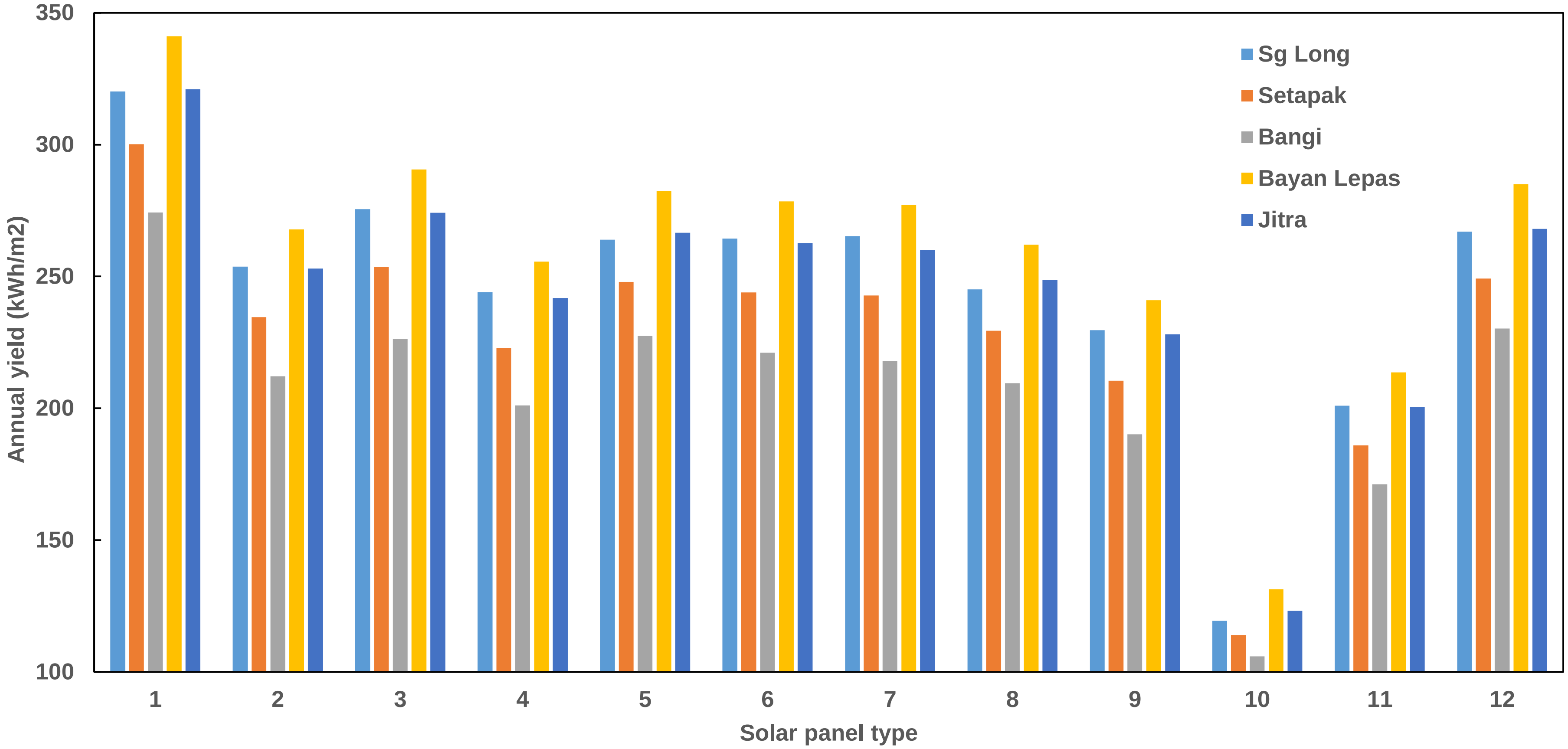

Figure 4.1: Annual energy yield by modules 1 to 12 at various locations

4.2 Results using MmGA and NSGAII

In addition to the effect of the solar radiance using SSGA, the experiments are expended using a multi-objective problem. A total of three objectives are defined, as follows:

1. PCE, where a higher value preferred,
2. Weight per output power, where a smaller value preferred,
3. Panel area per output power, where a smaller value preferred.

These objectives are optimized using two GA variants, i.e., MmGA and NSGAII. Optimization is done for the irradiance level at NOC, which is at 800 W/m^2. Results from Sg Long is first taken into account in Table 4.7. It can be seen that module type 3 offers the highest PCE, lowest weight and smallest panel area per output power.

Table 4.7: Multi-objective results for Sg Long

Type	Objective 1		Objective 2		Objective 3	
	MmGA	**NSGAII**	**MmGA**	**NSGAII**	**MmGA**	**NSGAII**
1	15.205%	15.205%	0.04758	0.04759	7.54836	7.54852
2	16.013%	16.013%	0.04165	0.04166	7.38629	7.38647
3	**17.365%**	**17.365%**	**0.02866**	**0.02867**	**6.87104**	**6.87118**
4	15.407%	15.407%	0.04631	0.04631	7.71364	7.71381
5	16.787%	16.787%	0.04214	0.04215	6.92905	6.92931
6	16.704%	16.704%	0.04333	0.04333	7.05268	7.05285
7	16.733%	16.733%	0.03553	0.03554	7.03360	7.03392
8	15.526%	15.526%	0.04445	0.04445	7.60620	7.60641
9	14.480%	14.480%	0.05807	0.05808	8.20402	8.20416
10	7.021%	7.138%	0.20861	0.22189	16.79640	17.86512
11	12.975%	12.975%	0.08987	0.08988	8.71392	8.71413
12	17.199%	17.199%	0.07136	0.07137	6.56512	6.56528

A similar pattern can be seen for the results from Setapak, with module type 3 having the best results, as listed in Table 4.8.

Table 4.8: Multi-objective results for Setapak

Type	Objective 1		Objective 2		Objective 3	
	MmGA	**NSGAII**	**MmGA**	**NSGAII**	**MmGA**	**NSGAII**
1	14.212%	14.212%	0.11251	0.11252	9.85811	9.85833
2	14.656%	14.656%	0.10513	0.10513	9.60485	9.60516
3	**15.792%**	**15.792%**	**0.07695**	**0.07695**	**8.96343**	**8.96379**
4	13.965%	13.965%	0.11367	0.11367	10.03643	10.03670
5	15.527%	15.527%	0.10123	0.10123	9.04019	9.04044
6	15.234%	15.234%	0.11141	0.11141	9.25595	9.25622
7	15.047%	15.047%	0.10793	0.10794	9.51164	9.51202
8	14.391%	14.391%	0.10442	0.10442	9.72669	9.72687
9	13.150%	13.150%	0.15068	0.15069	10.72312	10.72358
10	7.020%	7.140%	0.20834	0.22505	16.77470	18.11997
11	11.735%	11.735%	0.19715	0.19715	11.82881	11.82911
12	15.784%	15.784%	0.14555	0.14556	8.73317	8.73352

In the case of Bangi (Table 4.9), module type 12 had the best results for the highest PCE and smallest panel per output power. However, module type 3 had the lowest weight. As module type 12 had two of the three best objectives, module type 12 should be given the consideration.

Table 4.9: Multi-objective results for Bangi

Type	Objective 1		Objective 2		Objective 3	
	MmGA	**NSGAII**	**MmGA**	**NSGAII**	**MmGA**	**NSGAII**
1	13.943%	13.943%	0.09357	0.09357	8.19787	8.19800
2	14.263%	14.263%	0.08889	0.08889	8.12121	8.12143
3	15.223%	15.223%	**0.06612**	**0.06612**	7.70170	7.70194
4	13.516%	13.516%	0.09830	0.09830	8.67950	8.67973
5	15.288%	15.288%	0.08314	0.08314	7.42422	7.42444
6	14.866%	14.866%	0.09324	0.09324	7.74680	7.74695
7	14.650%	14.650%	0.08869	0.08869	7.81611	7.81629
8	14.088%	14.088%	0.08766	0.08766	8.16527	8.16550
9	12.789%	12.789%	0.12743	0.12743	9.06829	9.06855
10	7.141%	7.139%	0.22777	0.22293	18.33865	17.94894
11	11.513%	11.513%	0.16696	0.16696	10.01737	10.01753
12	**15.484%**	**15.484%**	0.12471	0.12472	**7.48278**	**7.48293**

Results from Bayan Lepas (Table 4.10) show a similar pattern as with the rest, with module type 3 coming out as the winner. Similarly, in Jitra (Table 4.11), module type 3 again emerged as the winner for all three objectives.

Table 4.10: Multi-objective results for Bayan Lepas

Type	Objective 1		Objective 2		Objective 3	
	MmGA	NSGAII	MmGA	NSGAII	MmGA	NSGAII
1	14.224%	14.224%	0.10031	0.10031	8.78872	8.78886
2	14.796%	14.796%	0.09257	0.09257	8.45740	8.45749
3	**16.056%**	**16.056%**	**0.06689**	**0.06689**	**7.79217**	**7.79226**
4	14.127%	14.127%	0.10029	0.10029	8.85519	8.85527
5	15.587%	15.587%	0.08981	0.08981	8.01986	8.01995
6	15.367%	15.367%	0.09791	0.09791	8.13476	8.13488
7	15.294%	15.294%	0.09275	0.09275	8.17372	8.17386
8	14.475%	14.475%	0.09280	0.09280	8.64445	8.64453
9	13.318%	13.318%	0.13201	0.13201	9.39463	9.39472
10	7.085%	7.139%	0.21963	0.22420	17.68325	18.05122
11	11.804%	11.804%	0.17639	0.17639	10.58321	10.58331
12	15.747%	15.747%	0.13229	0.13229	7.93733	7.93744

Table 4.11: Multi-objective results for Jitra

Type	Objective 1		Objective 2		Objective 3	
	MmGA	NSGAII	MmGA	NSGAII	MmGA	NSGAII
1	14.034%	14.034%	0.07343	0.07343	6.43362	6.43378
2	14.670%	14.670%	0.06542	0.06542	5.97712	5.97746
3	**15.992%**	**15.992%**	**0.04505**	**0.04506**	**5.24816**	**5.24840**
4	13.959%	13.959%	0.07237	0.07238	6.39038	6.39061
5	15.430%	15.430%	0.06516	0.06517	5.81906	5.81936
6	15.240%	15.240%	0.06927	0.06927	5.75520	5.75539
7	15.224%	15.224%	0.06158	0.06159	5.42719	5.42744
8	14.353%	14.353%	0.06736	0.06737	6.27492	6.27514
9	13.221%	13.221%	0.09288	0.09289	6.61008	6.61044
10	7.144%	7.141%	0.23131	0.22737	18.62358	18.30646
11	11.468%	11.468%	0.13849	0.13849	8.30924	8.30952
12	15.431%	15.431%	0.10649	0.10650	6.38970	6.38988

It can be seen that both MmGA and NSGAII results are quite similar, with some of the results from MmGA showing a lower value, especially for the third objective. In general, it can be seen that module type 3 (Sanyo HIT-H250E01) performs best in all three objectives for most of the locations, which would result optimum PCE with the lightest weight and smallest size.

CHAPTER 5

CONCLUSIONS

5.1 Conclusions

In this thesis, a comprehensive methodology for discussing the effects of local spectral irradiance on solar PV modules has been detailed. As a case study, 5 different locations in Malaysia were taken, with 12 types of solar modules. The actual performance of the solar cells at these specific locations was of interest. The baseline PCE referred to the AM1.5G, as given in the datasheet. From the experiments, it can be seen a big gap of PCE from the datasheet, as compared with different locations. The difference could be up to 15%, as compared to AM1.5G values. Based on the single objective results using GA, module type 1 (SunPower SPR-X21-345) at Bayan Lepas showed the best performance, in terms of PCE, yielding a total of 341 kWh/m2 of annual energy yield. When it came to the three objectives using MmGA and NSGAII, results shifted over to module type 3 (Sanyo HIT-H250E01) had the best results across all objectives in most of the locations.

Selecting the right module at the specific location is vital to maximize the energy yield. Lastly, this analysis provides the direction and guidance in selecting the most appropriate module that can perform best in the particular location to optimize the investment.

5.2 Future work

Future work will look into a more extensive selection of locations across Malaysia and a range of various solar panels. It is also envisioned to have a simple-to-use Android and iOS app for users to select the best panel for their location.

REFERENCES

Agapie, A., & Wright, A. H. (2014). Theoretical analysis of steady state genetic algorithms. *Applications of Mathematics*, *59*(5), 509-525.

Arias-Rosales, A., & Mejía-Gutiérrez, R. (2018). Optimization of V-Trough photovoltaic concentrators through genetic algorithms with heuristics based on Weibull distributions. *Applied Energy*, *212*, 122-140.

Bastidas-Rodriguez, J. D., Petrone, G., Ramos-Paja, C. A., & Spagnuolo, G. (2017). A genetic algorithm for identifying the single diode model parameters of a photovoltaic panel. *Mathematics and Computers in Simulation*, *131*, 38-54.

Blaifi, S., Moulahoum, S., Colak, I., & Merrouche, W. (2016). An enhanced dynamic model of battery using genetic algorithm suitable for photovoltaic applications. *Applied Energy*, *169*, 888-898.

Bucking, S., & Dermardiros, V. (2018). Distributed evolutionary algorithm for co-optimization of building and district systems for early community energy masterplanning. *Applied Soft Computing*, *63*, 14-22.

Burhan, M., Chua, K. J. E., & Ng, K. C. (2016). Sunlight to hydrogen conversion: Design optimization and energy management of concentrated photovoltaic (CPV-Hydrogen) system using micro genetic algorithm. *Energy*, *99*, 115-128.

Carotenuto, P. L., Della Cioppa, A., Marcelli, A., & Spagnuolo, G. (2015). An evolutionary approach to the dynamical reconfiguration of photovoltaic fields. *Neurocomputing*, *170*, 393-405.

Chong, K. K., Khlyabich, P. P., Hong, K. J., Reyes-Martinez, M., Rand, B. P., & Loo, Y. L. (2016). Comprehensive method for analyzing the power conversion efficiency of organic solar cells under different spectral irradiances considering both photonic and electrical characteristics. *Applied Energy*, *180*, 516-523.

Coello, C. A. C. C., & Pulido, G. T. (2001). A micro-genetic algorithm for multiobjective optimization. In *International Conference on Evolutionary Multi-Criterion Optimization* (pp. 126-140). Springer, Berlin, Heidelberg.

Coello, C. C., & Pulido, G. T. (2005). Multiobjective structural optimization using a microgenetic algorithm. *Structural and Multidisciplinary Optimization, 30*(5), 388-403.

Cortés, P., Muñuzuri, J., & Domínguez, I. (2018). Genetic algorithms to optimize the operating costs of electricity and heating networks in buildings considering distributed energy generation and storage. *Computers & Operations Research*.

Daraban, S., Petreus, D., & Morel, C. (2014). A novel MPPT (maximum power point tracking) algorithm based on a modified genetic algorithm specialized on tracking the global maximum power point in photovoltaic systems affected by partial shading. *Energy, 74*, 374-388.

De Soto, W., Klein, S. A., & Beckman, W. A. (2006). Improvement and validation of a model for photovoltaic array performance. *Solar Energy, 80*(1), 78-88.

Deb, K., Pratap, A., Agarwal, S., & Meyarivan, T. A. M. T. (2002). A fast and elitist multiobjective genetic algorithm: NSGA-II. *IEEE transactions on evolutionary computation, 6*(2), 182-197.

Dirnberger, D., Blackburn, G., Müller, B., & Reise, C. (2015). On the impact of solar spectral irradiance on the yield of different PV technologies. *Solar Energy Materials and Solar Cells, 132*, 431-442.

Efron, B. & Tibshirani, R. (1993). An Introduction to the Bootstrap, Chapman and Hall, New York.

Goldberg, D. E. (1989). Sizing populations for serial and parallel genetic algorithms. In *Proc. 3rd Int. Conf. on Genetic Algorithms* (pp. 70-79).

Holland, J. H. (1992). Adaptation in natural and artificial systems: an introductory analysis with applications to biology, control, and artificial intelligence. MIT press.

Horio, Y., Rahman, M. M., Imai, Y., Hishikawa, Y., & Minemoto, T. (2017). Impact of the average photon-energy coefficient of solar spectrum on the short circuit current of photovoltaic modules. *Current Applied Physics, 17*(10), 1341-1346.

Ishii, T., Otani, K., & Takashima, T. (2011). Effects of solar spectrum and module temperature on outdoor performance of photovoltaic modules in round-robin measurements in Japan. Progress in Photovoltaics: *Research and Applications, 19*(2), 141-148.

Jiménez-Fernández, S., Salcedo-Sanz, S., Gallo-Marazuela, D., Gómez-Prada, G., Maellas, J., & Portilla-Figueras, A. (2014). Sizing and maintenance visits optimization of a hybrid photovoltaic-hydrogen stand-alone facility using evolutionary algorithms. *Renewable Energy*, *66*, 402-413.

Kumari, P. A., & Geethanjali, P. (2017). Adaptive Genetic Algorithm Based Multi-Objective Optimization for Photovoltaic Cell Design Parameter Extraction. *Energy Procedia*, *117*, 432-441.

Ma, T., Yang, H., & Lu, L. (2017). Long-term performance analysis of a stand-alone photovoltaic system under real conditions. *Applied Energy, 201*, 320-331.

Mano, H., Rahman, M. M., Kamei, A., & Minemoto, T. (2017). Impact estimation of average photon energy from two spectrum bands on short circuit current of photovoltaic modules. *Solar Energy, 155*, 1300-1305.

Minemoto, T., Fukushige, S., & Takakura, H. (2009). Difference in the outdoor performance of bulk and thin-film silicon-based photovoltaic modules. *Solar Energy Materials and Solar Cells, 93*(6-7), 1062-1065.

Muhsen, D. H., Ghazali, A. B., Khatib, T., & Abed, I. A. (2015). Parameters extraction of double diode photovoltaic module’s model based on hybrid evolutionary algorithm. *Energy Conversion and Management, 105*, 552-561.

Muhsen, D. H., Ghazali, A. B., Khatib, T., & Abed, I. A. (2016). A comparative study of evolutionary algorithms and adapting control parameters for estimating the parameters of a single-diode photovoltaic module's model. *Renewable energy*, *96*, 377-389.

Muneer, T. (2007). Solar radiation and daylight models. Routledge.

National Renewable Energy Policy & Action Plan (2017), Sustainable Energy Development Authority Malaysia.

Nofuentes, G., Gueymard, C. A., Aguilera, J., Pérez-Godoy, M. D., & Charte, F. (2017). Is the average photon energy a unique characteristic of the spectral distribution of global irradiance?. *Solar Energy, 149*, 32-43.

Norton, M., Amillo, A. G., & Galleano, R. (2015). Comparison of solar spectral irradiance measurements using the average photon energy parameter. *Solar Energy, 120*, 337-344.

Paulitschke, M., Bocklisch, T., & Böttiger, M. (2017). Comparison of particle swarm and genetic algorithm based design algorithms for PV-hybrid systems with battery and hydrogen storage path. *Energy Procedia*, *135*, 452-463.

Rong, J., Wang, B., Liu, B., & Zha, X. (2015). Parameter Optimization of PV based on Hybrid Genetic Algorithm. *IFAC-PapersOnLine*, *48*(28), 568-572.

Senthilarasu, S., Fernández, E. F., Almonacid, F., & Mallick, T. K. (2015). Effects of spectral coupling on perovskite solar cells under diverse climatic conditions. *Solar Energy Materials and Solar Cells, 133*, 92-98.

Shirzadi, S., Hizam, H., & Wahab, N. I. A. (2014). Mismatch losses minimization in photovoltaic arrays by arranging modules applying a genetic algorithm. *Solar Energy*, *108*, 467-478.

Siddiqui, M. U., & Abido, M. (2013). Parameter estimation for five-and seven-parameter photovoltaic electrical models using evolutionary algorithms. *Applied Soft Computing*, *13*(12), 4608-4621.

Singh, S., & Agrawal, S. (2015). Parameter identification of the glazed photovoltaic thermal system using Genetic Algorithm–Fuzzy System (GA–FS) approach and its comparative study. *Energy Conversion and Management*, *105*, 763-771.

Singh, S., & Agrawal, S. (2016). Efficiency maximization and performance evaluation of hybrid dual channel semitransparent photovoltaic thermal module using fuzzyfied genetic algorithm. *Energy conversion and management*, *122*, 449-461.

Singh, S., Agarwal, S., Tiwari, G. N., & Chauhan, D. (2015). Application of genetic algorithm with multi-objective function to improve the efficiency of glazed photovoltaic thermal system for New Delhi (India) climatic condition. *Solar Energy*, *117*, 153-166.

Singh, S., Agrawal, S., & Gadh, R. (2015). Optimization of single channel glazed photovoltaic thermal (PVT) array using Evolutionary Algorithm (EA) and carbon credit earned by the optimized array. *Energy Conversion and Management*, *105*, 303-312.

Singh, S., Agrawal, S., Tiwari, A., Al-Helal, I. M., & Avasthi, D. V. (2015). Modeling and parameter optimization of hybrid single channel photovoltaic thermal module using genetic algorithms. *Solar Energy*, *113*, 78-87.

Sirisamphanwong, C., & Ketjoy, N. (2012). Impact of spectral irradiance distribution on the outdoor performance of photovoltaic system under Thai climatic conditions. *Renewable Energy, 38*(1), 69-74.

Tan, C. J., Hanoun, S., & Lim, C. P. (2015). A multi-objective evolutionary algorithm-based decision support system: A case study on job-shop scheduling in manufacturing. In *Systems Conference (SysCon), 2015 9th Annual IEEE International* (pp. 170-174). IEEE.

Tan, C. J., Lim, C. P., & Cheah, Y. N. (2013). A modified micro genetic algorithm for undertaking multi-objective optimization problems. *Journal of Intelligent & Fuzzy Systems*, *24*(3), 483-495.

Vavak, F., & Fogarty, T. C. (1996). Comparison of steady state and generational genetic algorithms for use in nonstationary environments. In *Evolutionary Computation, 1996, Proceedings of IEEE International Conference on* (pp. 192-195). IEEE.

Youssef, A. M. A., Zhai, Z. J., & Reffat, R. M. (2016). Genetic algorithm based optimization for photovoltaics integrated building envelope. *Energy And Buildings*, *127*, 627-636.